Research Article

Simplified Analytical Method for Estimating the Resistance of Lock Gates to Ship Impacts

Loïc Buldgen,[1] Hervé Le Sourne,[2] and Philippe Rigo[1]

[1] *Faculty of Applied Sciences and ANAST, University of Liège, 1 Chemin des Chevreuils,*
4000 Liège, Belgium
[2] *Mechanical Engineering Department (LE2M), ICAM Nantes Campus,*
35 avenue du Champ de Manœuvres, 44470 Carquefou, France

Correspondence should be addressed to Loïc Buldgen, l.buldgen@ulg.ac.be

The present paper is concerned with the design of lock gates submitted to ship impacts. In this paper, a simplified analytical method is presented to evaluate the resistance of such structures under collision. The basic idea is to assume that the resistance is first provided through a local deforming mode, corresponding to a localized crushing of some impacted structural elements. For consecutive larger deformations, the resistance is then mostly provided through a global deforming mode, corresponding to an overall movement of the entire gate. For assessing the resistance in the case of the local deforming mode, the structure is divided into a given number of large structural entities called "superelements." For each of them, a relation between the resistance of the gate and the penetration of the striking ship is established. However, as some results are already available in the literature, this subject is not treated extensively in this paper. On the contrary, the calculation of the resistance of the gate provided through the global mode is detailed and the strategy to switch from local to global deformation is highlighted. Finally, we propose to validate our developments by making a comparison between results obtained numerically and those predicted by the present analytical approach.

1. Introduction

Amongst all the loads that have to be expected for the design of lock gates, the collision of a vessel is one of the most difficult to handle.

A collision may result in some minor damages to the plating or to the stiffening system of the gate, producing, for example, a local loss of water tightness. However, if the initial velocity of the striking ship is large enough, the displacements imposed to the structure may cause a complete collapse of the gate. This would result in the emptying of the damaged reach, with probably the complete sinking of the striking ship.

To deal properly with ship impact, it is of course possible to use nonlinear finite element methods. Nevertheless, at the predesign stage of a gate, such approaches are rather restrictive because of the time required to model and simulate collisions. Therefore, we propose here to establish an analytical simplified method in order to verify the resistance of gates submitted to a ship impact.

For the moment, the development of such simplified methods is not really reported in the literature. Some very interesting results have been established for the purpose of analyzing collisions between two ships. For example, the crushing resistance of web girders has already been theoretically and experimentally studied by Wierzbicki and Culbertson Driscoll [1], Wang and Ohtsubo [2], Simonsen [3], Zhang [4], and Hong and Amdahl [5]. Each of them developed analytical formulations that may be useful for studying locally the contact between a ship and a gate.

Additional results are also available for impacted panels, which have been investigated in detail by Wang [6], Wang and Ohtsubo [7], and Zhang [8]. Some references are also useful for evaluating the resistance of metal plates after rupture, when they are submitted to tearing and cutting. For example, these phenomena have been studied by Wang and Ohtsubo [7], Zhang [8], Wierzbicki [9], and Zheng [10]. In the particular case of stiffened panels subjected to lateral loads, the developments performed by Paik [11], Cho and Lee [12], or Ueda et al. [13] constitute a very accurate basis for performing analytical estimation of the resistance of such structural components.

The previous brief literature review shows that some results are already available to deal with a simplified approach of collisions between ships and gates. All these developments constitute of course an invaluable help for developing simplified collision models of lock gates, but they are not sufficient. The principal reason is that the behavior of an impacted gate may not directly be assimilated to the one of an impacted vessel. Consequently, some researches in this domain are still needed.

The aim is to develop some analysis tools, which would be time and cost-effective in the predesign stage of gates. To achieve this goal, we will follow a similar method to the one proposed by Le Sourne et al. [14]. The basic idea is that the total resistance of the struck gate is provided by two deforming modes:

(i) the *local* one, which implies a local crushing of all the impacted structural elements;

(ii) the *global* one, which supposes an overall deformation of the gate.

In the present paper, we try to go further into this philosophy.

2. General Description of the Problem

In this paper, we consider the exceptional situation of ship colliding with a lock gate. The collision scenario is depicted in Figure 1, where the general coordinate system is denoted by (X, Y, Z). For avoiding confusion in the present paper, we will use the terminology "transversal," "vertical," and "longitudinal" in accordance with the respective orientation of X, Y, and Z axes.

In our scenario, the vessel is coming from upstream, and, consequently, the impact is located on the downstream gate of the lock. It is clear that this case is the least desired because the hydrostatic pressure is acting in the same direction as the impact force. On the contrary, if the collision was happening in the downstream reach of the lock, the resulting hydrostatic pressure would act in opposition with the impact force and would compensate it partially.
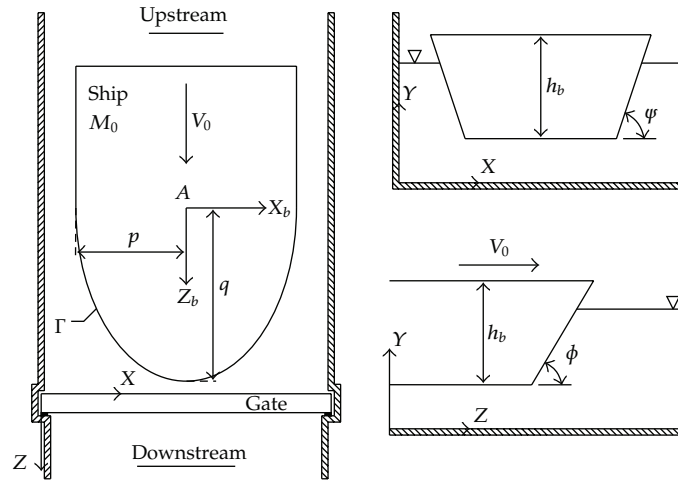
Figure 1: Plane and section views of the impact situation.

In order to derive an analytic procedure for estimating the collision resistance of the gate, we first need to describe the ship and the gate using various parameters. This is the purpose of the subsequent sections.

2.1. Geometrical Description of the Striking Vessel

The vessel is characterized through the following: mass M_0 and velocity V_0. In other words, we assume a certain kinetic energy $M_0 V_0^2 / 2$ for the striking ship. These two parameters are chosen according to the waterway class, which determines the maximal speed as well as the allowable shipping of the vessels.

From the geometric point of view, we first assume that the shape of the bow at the uppermost deck may be fairly modeled by a parabola Γ (see Figure 1) having a transversal radius p and a longitudinal radius q. Consequently, in the local axes (x_b, z_b) positioned in point A, the equation of the curve Γ is given by

$$\Gamma \equiv z_b = q \cdot \left(1 - \frac{x_b^2}{p^2} \right). \tag{2.1}$$

In order to have a global description of the geometry of the ship, it is also required to introduce the following parameters (see also Figure 1):

(i) the height h_b between the uppermost deck and the bottom of the ship;

(ii) the side angle ψ and the stem angle ϕ, which are used to fix the inclination of the bow.

It is important to note that all the above mentioned properties are required input data, which have to be provided by the user before the beginning of the calculation process.
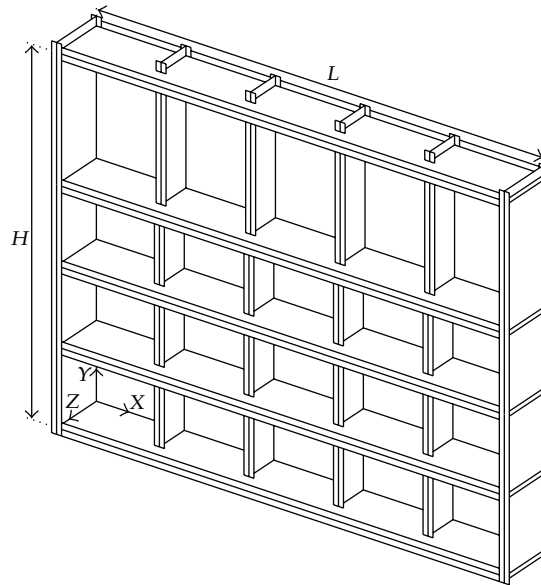
Figure 2: Three-dimensional representation of the considered type of gate.

2.2. Description of the Gate

In this paper, we will only focus on gates with a single plating. A three-dimensional picture of such a structure is depicted in Figure 2, where the notations H and L are used for representing, respectively, the total vertical and the total transversal extension of the gate. In fact, these gates are rather similar to large orthotropic plates, constituted by a plating (for retaining water) stiffened by the following elements (see Figures 2 and 3):

   (i) the transversal frames, which may be seen as beams presenting a T-shaped cross-section; they are placed in the transversal direction (i.e., along the X axis);

   (ii) the vertical frames, which are also beams with a T-shaped cross-section but are arranged in the vertical direction (i.e., along the Y axis);

   (iii) the stiffeners, which are optional reinforcing beams disposed transversally on the plating in order to avoid instabilities in shells; their cross-section may exhibit various shapes.

The geometric data required for characterizing the stiffening system are mainly the dimensions of the different cross-sections. As shown in Figure 3, the needed values are the height h_w and thickness t_w of the web, as well as the height h_f and thickness t_f of the flange. For the plating, it is only necessary to precise its thickness t_p. With all these parameters and knowing the properties of the material constituting the gate, it is possible to derive the mechanical properties of all the stiffening elements.

Another point that has to be clarified concerns the assumed support conditions of the structure. When the gate is closed, the contact is supposed to be established against the support denoted by S_1, S_2, and S_3 in Figure 3, and, consequently, we may admit that:

   (i) the gate is simply applied against the two lock walls (supports S_1 and S_2 in Figure 3). The translational degree of freedom in the Z direction has therefore to be blocked along the all vertical extensions of the gate in S_1 and S_2;
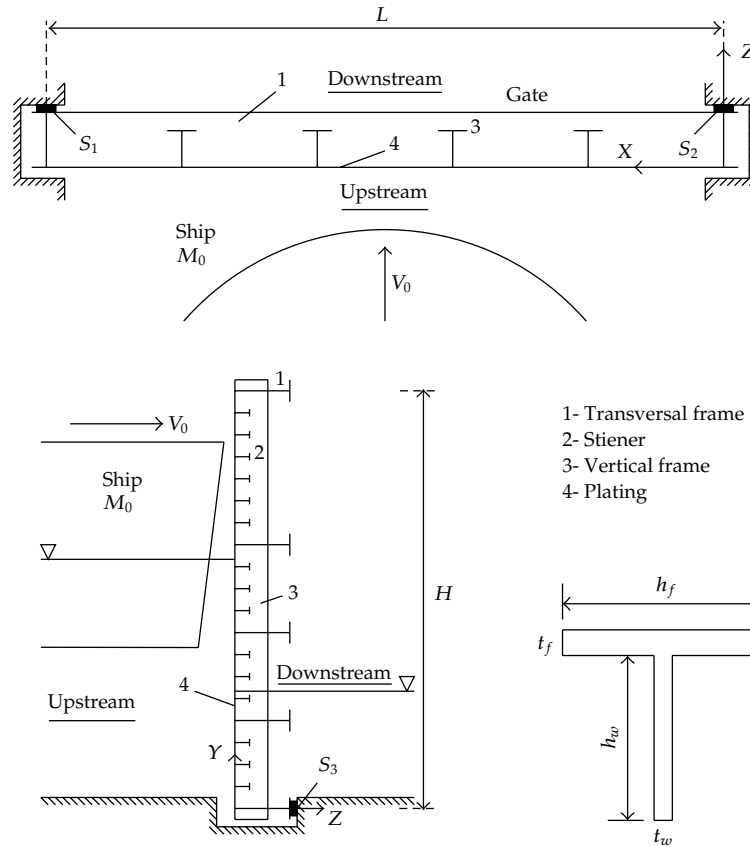
Figure 3: Plan and section views of the gate.

(ii) the gate is simply applied against the sill located at the bottom of the chamber (support S_3 in Figure 3). Therefore, it seems to be reasonable to restrain the translational displacement in the Z direction along the all transversal extension of the gate in S_3.

2.3. Description of the Material

The present paper is concerned with the resistance of a lock gate impacted by a ship. The primary goal is not to assess the damages caused to the vessel: we are much more interested in the ability aspect of the structural resistance to collisions. As a consequence, we assume that the material constituting of the striking vessel is infinitely rigid. In other words, we will not allow any deformation in the ship structure, which is a conservative approach in the evaluation of the resistance.

On the contrary, the previous hypothesis is not valid for the gate as it is supposed to be deformable. Nowadays, the most common material used for such structures is construction steel, so we will only deal with this material in the present paper. This kind of steel exhibits
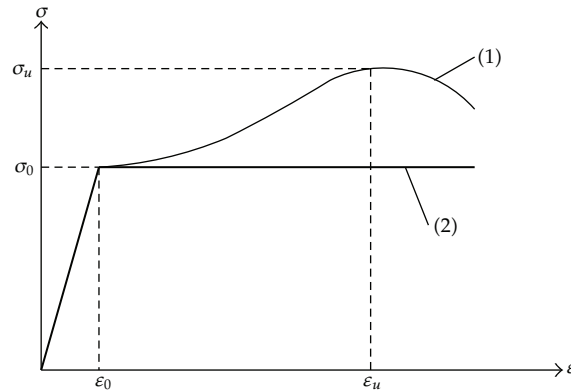
Figure 4: Real (1) and idealized (2) constitutive law of standard construction steel.

a constructive law represented by curve (1) in Figure 4 and may be defined by the following parameters:

(i) the maximal elastic stress σ_0, with which is associated the maximal elastic deformation ϵ_0;

(ii) the rupture stress σ_u, for which tearing is observed in the material; the corresponding deformation is called ϵ_u;

(iii) Young's modulus E characterizing the stiffness of the material during the elastic phase.

In order to simplify the analytical derivation of the collision resistance, we will suppose here that the steel has a so-called elastic-perfectly plastic behavior. This means that the relation between stresses and strains is idealized by curve (2) in Figure 4. Consequently, we neglect the additional resistance coming from hardening of steel, which is in fact a conservative assumption.

2.4. General Positioning in the Space

To define the collision scenario, it is still necessary to position the resistance element as well as the striking ship within the area of space. To do so, different kinds of input data are still required:

(i) the impact point E, that is, the point of the gate where the first contact between the bow and the plating will be established; this point is located by its coordinate (X_E, Y_E), as shown in Figures 5 and 6;

(ii) the transversal positions X_i of the vertical frames, that is, the position of each vertical frame along the X axis (see Figure 5);

(iii) the vertical positions Y_i of the horizontal frames, that is, the position of each horizontal frame along the Y axis (see Figure 5);

(iv) the total number of stiffeners distributed along the vertical height H of the gate.

When all the previous inputs are placed, the three-dimensional configuration of the gate is completely defined.
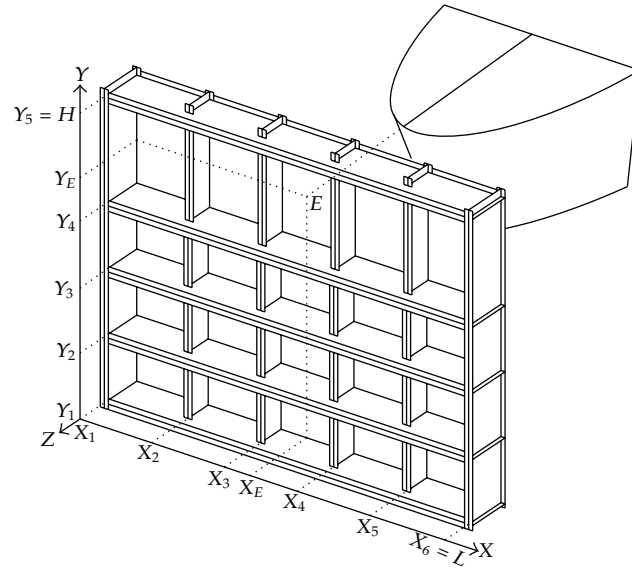
Figure 5: Position of the resistance elements and of the impact point.

3. Methodology for Evaluating the Collision Resistance

3.1. General Principles

When a ship collides with a gate, its action on the impacted structure may be represented by a force P_t acting in the same direction as the indentation δ of the striking vessel (see Figure 6). By equilibrium, this force may be seen as the resistance opposed by the gate to the progression of the ship. Therefore, the goal of our work is to assess the value of P_t for a given indentation δ of the vessel. In other words, our aim is to derive the evolution of P_t with δ by means of simplified analytical procedures.

When a ship is entering into a lock, it seems reasonable to admit that its initial velocity V_0 is quite small. Consequently, the dynamic effects in the gate remain moderate, and we may assume that the initial kinetic energy $M_0 V_0^2/2$ of the ship is entirely dissipated by deformation of the impacted gate E_{int}, that is,

$$\frac{1}{2} M_0 V_0^2 = E_{\text{int}}. \tag{3.1}$$

Knowing the relation between P_t and δ, it is possible to calculate E_{int} simply by integration (see Figure 7):

$$E_{\text{int}} = \int_0^{\delta_{\max}} P_t(\delta) \cdot d\delta. \tag{3.2}$$
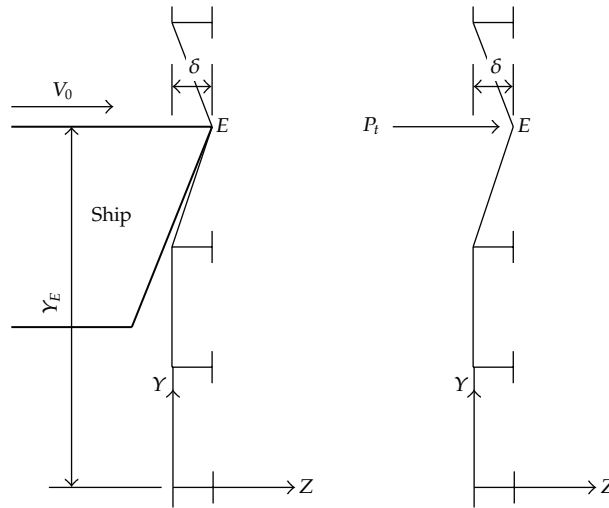
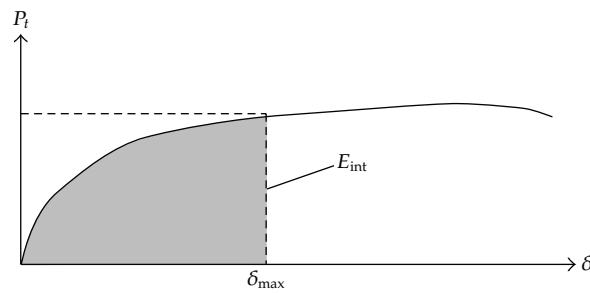**Figure 6:** Representation of the impact force.

Figure 7: Evolution of the resistance of the gate with the penetration of the ship.

For a given ship of mass M_0 and velocity V_0, (3.1) and (3.2) give the maximal penetration $\delta_{\max}$, which has to be supported by the gate to withstand an impact with such a vessel. According to the maximal degradation level accepted for the gate, it can be decided if this value of $\delta_{\max}$ may be applicable or not.

3.2. Theoretical Basis

The theoretical basis for deriving $P_t(\delta)$ is the so-called *upper-bound theorem*, which states that *"if the work rate of a system of applied loads during any kinematically admissible collapse of a structure is equated to the corresponding internal energy dissipation rate, then that system of loads will cause collapse, or incipient collapse, of the structure."*

In the present case, it is obvious that the external dissimilation rate $\dot{E}_{\mathrm{ext}}$ is entirely produced by the force P_t applied by the ship on the gate. Therefore, we have

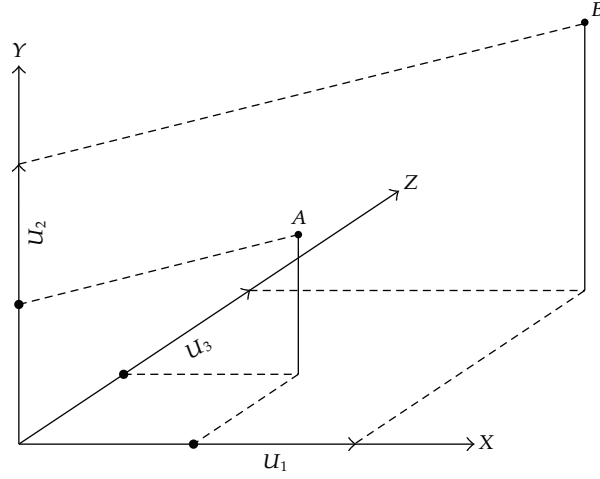$$\dot{E}_{\mathrm{ext}} = P_t V_0 = P_t \dot{\delta}, \tag{3.3}$$

Figure 8: Definition of the displacement field.

where $(\dot{\ }) = \partial/\partial t$ is the derivative with respect to time. On the other hand, if we neglect the dynamic effects in the structure, the internal dissipation rate $\dot{E}_{int}$ is entirely coming from the deformation of the gate. If $\mathcal{V}$ is the total volume of the structure, using Einstein's notation we have:

$$\dot{E}_{int} = \iiint_{\mathcal{V}} \sigma_{ij}\dot{e}_{ij}dX\,dY\,dZ, \tag{3.4}$$

where σ_{ij} and $\dot{e}_{ij}$ are, respectively, the stress and the strain rate tensors defined over the entire volume $\mathcal{V}$ of the gate. By application of the upper-bound theorem, we have

$$\dot{E}_{ext} = \dot{E}_{int} \implies P_t = \frac{1}{\dot{\delta}}\iiint_{\mathcal{V}} \sigma_{ij}\dot{e}_{ij}dX\,dY\,dZ. \tag{3.5}$$

Consequently, (3.5) may be useful for deriving $P_t(\delta)$, provided that we are able to establish a relation between the deformation rate $\dot{e}_{ij}$ and the velocity $\dot{\delta}$. To do so, we need to define the displacements over the entire volume $\mathcal{V}$. For example, in Figure 8, if we suppose that point A is moving to point B for a given value of δ, we may define the three components $U_1(X,Y,Z,\delta)$, $U_2(X,Y,Z,\delta)$, and $U_3(X,Y,Z,\delta)$ of the displacement field along axis X, Y, or Z, respectively. Note that in the remaining part of this paper, we will also use the equivalent notations (U,V,W) and (X_1,X_2,X_3) for designating (U_1,U_2,U_3) and (X,Y,Z).

Using the Green-Lagrange tensor, it is finally possible to find a link between the deformation and the penetration of the ship δ:

$$e_{ij} = \frac{1}{2}\left(\frac{\partial U_i}{\partial X_j} + \frac{\partial U_j}{\partial X_i} + \frac{\partial U_k}{\partial X_i}\frac{\partial U_k}{\partial X_j}\right). \tag{3.6}$$

Equation (3.6) may be rewritten in the following shorter form:

$$\epsilon_{ij} = f_{ij}(X, Y, Z, \delta) \Longleftrightarrow \dot{\epsilon}_{ij} = \frac{\partial f_{ij}}{\partial \delta} \dot{\delta}. \tag{3.7}$$

If we want to apply formula (3.5) to obtain a relation between P_t and δ, it is also required to evaluate the stresses σ_{ij} as a function of δ. This may be achieved using the constitutive laws giving a relation between σ_{ij} and ϵ_{ij}. As the evolution of ϵ_{ij} with δ is known by (3.6), we also have

$$\sigma_{ij} = g_{ij}(X, Y, Z, \delta). \tag{3.8}$$

Note that U_1, U_2, and U_3 are unknown; for a given value of δ, we have to *postulate* a certain displacement field. Provided that this displacement field is kinematically admissible, we may apply the upper-bound theorem and calculate the resistance P_t with formula (3.5). In fact, if we combine (3.7) and (3.8) in (3.5), we obtain

$$P_t = \iiint_{\mathcal{V}} g_{ij}(X, Y, Z, \delta) \frac{\partial f_{ij}}{\partial \delta} dX\, dY\, dZ. \tag{3.9}$$

Equation (3.9) is the needed relation between P_t and δ. However, the crucial point in the above-described approach is to define properly a kinematically admissible displacement field, otherwise the upper-bound theorem may lead to an overestimation of the crushing resistance.

3.3. The Superelements Method

The integration of (3.9) has to be performed over the whole volume $\mathcal{V}$ of the struck structure and is rather impossible to derive analytically. As a consequence, we need to simplify the procedure described here over, and this may be achieved by splitting the gate into superelements.

The basic idea is to divide the gate into different substructures (the so-called superelements) that we assume working independently. For the lock gate depicted in Figure 2, the structure may be decomposed into two types of superelements.

(i) The first superelement (SE1) is a rectangular plate simply supported on its four edges and impacted perpendicularly to its plane, undergoing therefore important out-of-plane displacements. Such elements are typically used for modeling the plating of the gate.

(ii) The second superelement (SE2) is a beam with a T-shaped cross-section, impacted in its plane. This kind of element is therefore quite relevant for modeling transversal and horizontal frames.

The division of the gate into superelements is only based on geometric considerations. In order to illustrate this process, we can consider, for example, only a small part of the lock gate represented in Figure 2, for which the division principle is shown in Figure 9. As it can be seen, the two previous types of elements are sufficient for analyzing the structure.
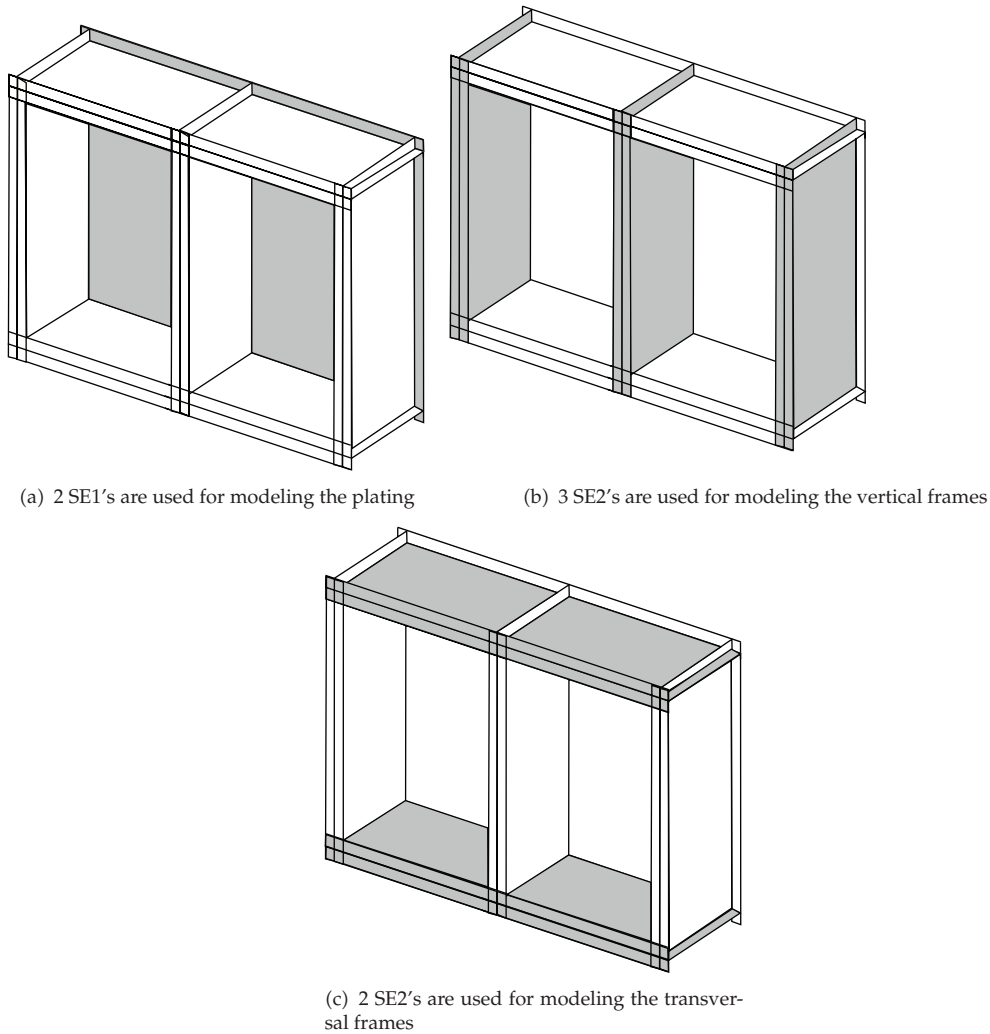
(a) 2 SE1's are used for modeling the plating

(b) 3 SE2's are used for modeling the vertical frames

(c) 2 SE2's are used for modeling the transversal frames

Figure 9: Illustration of the subdivision of a structure into superelements.

As long as there is no contact between the ship and a given superelement, this latter will remain inactive. This means that it will not deform until it has been collided by the bow, which is a consequence of the above-mentioned hypothesis that each substructure is working independently. After being activated, the superelement will deform and dissipate a certain amount of energy. If the gate is divided into n superelements, as each of them is decoupled from the others, the total internal energy E_{int} is simply obtained by summation of the individual contributions coming from the n superelements, that is,

$$E_{\text{int}} = \sum_{k=1}^{n} E_{\text{int}}^{(k)} \implies \dot{E}_{\text{int}} = \sum_{k=1}^{n} \dot{E}_{\text{int}}^{(k)}, \quad k \in \{1, \dots, n\}, \tag{3.10}$$

where $E_{\text{int}}^{(k)}$ is the internal energy dissipated by superelement number k for a given penetration δ of the ship. Before using (3.10), it is preliminary required to know $\dot{E}_{\text{int}}^{(k)}$. To do so, formula (3.4) is still valid, but it has to be reequated for the case of superelement k:

$$\dot{E}_{\text{int}}^{(k)} = \iiint_{\mathcal{V}_k} \sigma_{ij}^{(k)} \cdot \dot{\epsilon}_{ij}^{(k)} \cdot dX \, dY \, dZ, \quad k \in \{1, \dots, n\}, \tag{3.11}$$

where we have introduced the following notations:

  (i) $\sigma_{ij}^{(k)}$ is the stress tensor defined on the entire volume of superelement k,

  (ii) $\dot{\epsilon}_{ij}^{(k)}$ is the strain rate tensor defined on the entire volume of superelement k,

  (iii) $\mathcal{V}_k$ is the volume of superelement k.

By following a similar reasoning as for relations (3.7) and (3.8), we get finally the particularization of (3.9):

$$P_t^{(k)} = \iiint_{\mathcal{V}_k} g_{ij}^{(k)} \cdot \frac{\partial f_{ij}^{(k)}}{\partial \delta} \cdot dX \, dY \, dZ \implies P_t = \sum_{k=1}^{n} \iiint_{\mathcal{V}_k} g_{ij}^{(k)} \cdot \frac{\partial f_{ij}^{(k)}}{\partial \delta} \cdot dX \, dY \, dZ, \tag{3.12}$$

where $P_t^{(k)}$ may be seen as the contribution of superelement k to the total resistance of the gate (note that Einstein's notation has been used for the subscripts i and j). In fact, relation (3.12) is of primary importance because it constitutes the fundamental basis of the present method. Of course, we still need to develop adequately the functions involved in this expression. This will be done later for SE1 and SE2.

3.4. Global and Local Deforming Modes

We previously assumed that each superelement was working independently from the others. This hypothesis remains valid as long as the penetration δ is reasonably minor. However, when the penetration δ of the ship is increasing, deformations will occur in superelements that still have not been undertaken by the bow. Consequently, the internal energy rate for superelement k may not be equal to zero, although it has not been activated. This may be seen on Figure 10, where out-of-plane displacements occur in the entire gate, even if some regions have not been impacted by the striking ship bow.

In order to take this coupling into account, let us introduce the concept of local and global deforming modes.

  (i) We say that the structure exhibits a local deforming mode (see Figure 10) when the developments performed in Section 3.3 may be applied. In other words, we suppose here that the penetration of the vessel into the gate is only allowed by the local deformations of the activated superelements. Only the area impacted by the ship contributes to the energy dissipation; the other parts of the gate remain undeformed. Of course, it may be easily understood that the local mode is only valid for quite small values of δ.

  (ii) On the contrary, we say that the structure exhibits a global deforming mode (see Figure 10) when the displacements are not confined in a small area located around
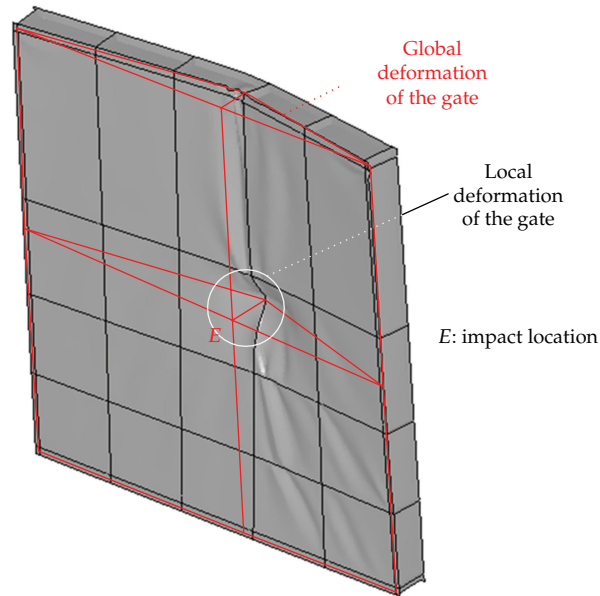
Figure 10: Illustration of global and local deformations.

the impact point. In this case, the entire gate is involved in the energy dissipation process and we may no longer assume that it behaves like a set of independent substructures activated progressively. Consequently, the superelements method is not valid anymore and the resisting force P_t has to be evaluated by another way than the one discussed in Section 3.3. This is precisely the topic of Section 5.

In order to model the phenomena depicted in Figure 10, we suppose that there is a sudden switch between the two modes. At the beginning, when the striking ship starts moving into the gate, the resistance P_t is essentially provided by the local deforming mode. This statement remains valid as long as the penetration δ does not exceed a transition value δ_t, for which the global mode is activated. In fact, the switch between the two modes occurs when the force P_t applied by the ship on the gate is sufficient to cause an overall displacement of the whole structure. As soon as $\delta \leq \delta_t$ two different values for P_t are computed:

(i) the value of P_t obtained by supposing a local deforming mode; it is denoted by P_{loc};

(ii) the value of P_t obtained by supposing a global deforming mode; it is denoted by P_{glob}.

For a given penetration δ, P_{loc} and P_{glob} are then compared. As long as $P_{\text{loc}} < P_{\text{glob}}$, the force exerted locally by the ship is not sufficient to cause an overall displacement of the gate, so the ship continues penetrating into the structure by local indentation. However, as soon as $P_{\text{loc}} = P_{\text{glob}}$, the force becomes sufficient and the switch from the local mode to the global one is obtained. The corresponding value of δ is the required δ_t (see Figure 11). After that, for the values of δ greater than δ_t, the resistance P_t is evaluated using equations specially developed for the global mode (see Section 5).
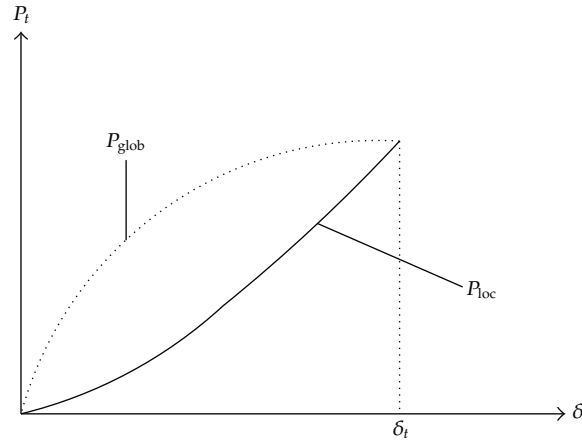
Figure 11: Evaluation of the transition from the local to the global mode.

4. Evaluation of the Resistance in the Local Deforming Mode

In the local deforming mode, the resistance of the gate is given by (3.12), where we assume that the total resisting force is simply obtained by adding the individual contributions of all the activated substructures. In this section, the laws governing the behavior of the two types of superelements introduced in Section 3.3 are detailed. However, as this topic is already well treated in the literature (see e.g., [4]), in order to avoid any redundancy, we have made a quite concise presentation of our approach.

Note

In the two following sections, we will use the superscript (k) for characterizing any property of the superelement number k.

4.1. Superelement Type 1 (SE1)

The first superelement is used for modeling the plating of the lock gate. Its boundaries are defined by the surrounding transversal and vertical frames, as shown in Figure 12. Considering the location of the impact point E, it is possible to fix the four parameters $a_1^{(k)}$, $a_2^{(k)}$, $b_1^{(k)}$, and $b_2^{(k)}$.

The thickness of the plate is equal to the thickness t_p of the plating. However, a correction is needed for taking into account the horizontal stiffeners placed in the transversal direction. During the collision, the stiffeners are mainly submitted to an axial extension; they will deform along the X direction by exhibiting a membrane behavior. Consequently, the plate thickness has to be modified for taking these effects into account. If A_s is the total area of all the stiffeners connected to the superelement k (see Figure 13), then we obtain

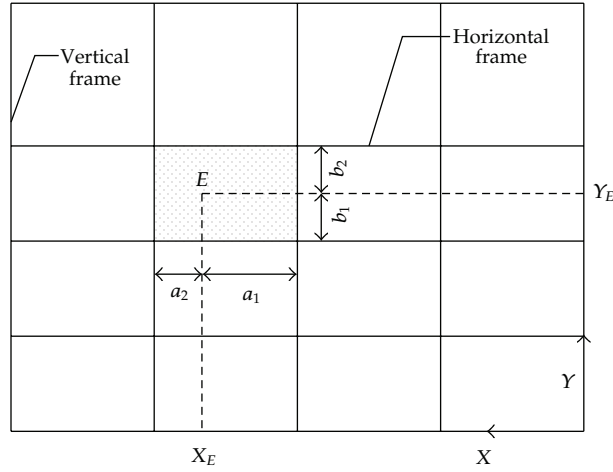$$t_X^{(k)} = t_p + \frac{A_s^{(k)}}{b_1^{(k)} + b_2^{(k)}}. \tag{4.1}$$

Figure 12: Definition of the main dimensions of SE1.
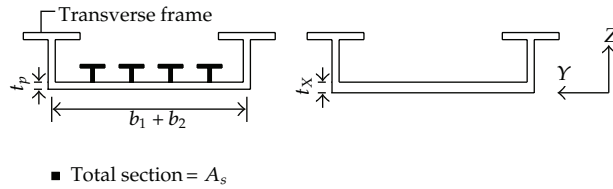

■ Total section = A_s

Figure 13: Equivalent plate thickness.

This correction has to be applied for the calculation of membrane effects in the X direction. However, if we consider membrane effects in the Y direction, the stiffeners have no influence and they do not need to be considered. Consequently, we have $t_Y^{(k)} = t_p$ and the plate becomes orthotropic.

In the present approach, we suppose that the impacted plate is completely independent from the surrounding other superelements. Therefore, it is acceptable to consider the plate as simply supported on its four edges. For a given indentation δ, the superelement will undergo mostly a membrane deformation; the effects of bending remain negligible.

When superelement SE1 is impacted by the bow of the vessel, for a given value of δ, we may deduct the deformation pattern shown in Figure 14. With this displacements field, it is possible to evaluate the internal energy rate, which has already been done by Zhang [4].

For the situation illustrated in Figure 14, Zhang [4] found the following crushing resistance for superelement k:

$$P_t^{(k)} = \frac{\sigma_0}{2\sqrt{3}} \left(a_1^{(k)} + a_2^{(k)} \right) \left(b_1^{(k)} + b_2^{(k)} \right) \left(\frac{t_X^{(k)}}{a_1^{(k)} a_2^{(k)}} + \frac{t_Y^{(k)}}{b_1^{(k)} b_2^{(k)}} \right). \tag{4.2}$$
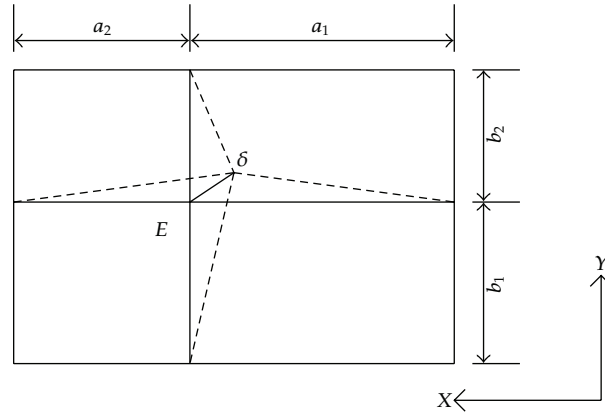
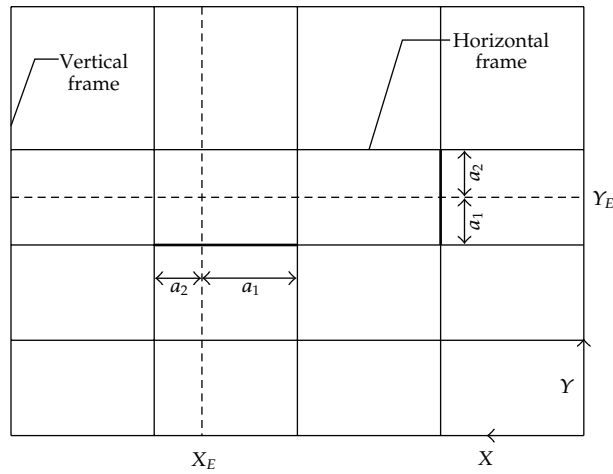**Figure 14:** Displacement field assumed for SE1.

Figure 15: Definition of the main dimensions of SE2.

4.2. Superelement Type 2 (SE2)

The second superelement that we will consider is used for modeling the transversal and vertical frames. The boundaries of a horizontal superelement are defined by the two adjacent vertical frames (and inversely for a vertical superelement).

The principal dimensions $a_1^{(k)}$ and $a_2^{(k)}$ (see Figure 15) of superelement k are positioned in accordance with the location of the impact point. The resisting cross-section has a T-shape, whose properties are defined in the general geometry of the gate.

When this superelement is impacted, we suppose that it will deform like a concertina. To do so, three plastic hinges are formed. They are designated by ABF, ACF, and ADF in Figure 16. These lines allow for relative rotation between the triangular surfaces ABC, ACD, BCF, and FCD. Bending effects are therefore preponderant along these lines.

However, the rotational movement of the triangular surfaces is not free because it must respect the compatibility between surfaces ABD and BFD along their common line BD. Therefore, surfaces ABD and BFD are submitted to an axial extension implying
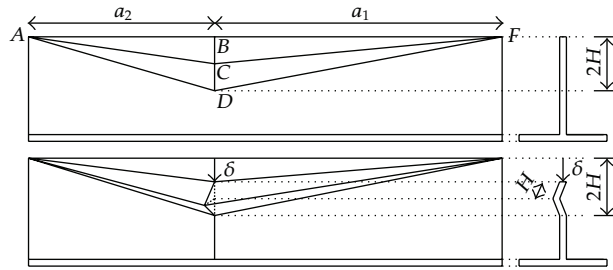
Figure 16: Displacements field assumed for SE2.

mainly membrane effects. Consequently, for a given indentation δ, the web will be folded as represented in Figure 16, where $2H$ is the total height of one fold. According to the previous hypothesis, during this motion, the energy is absorbed by membrane extension of the triangular regions ABD and BFD, but also by bending effects in the three plastic hinges ABF, ACF, and ADF. The phenomenon of concertina folding has already been studied by a great number of authors. For example, it was theoretically and experimentally studied by Wierzbicki and Culbertson Driscoll [1], Wang and Ohtsubo [2], Simonsen [3], and Zhang [4]. Hong and Amdahl [5] compared all these various approaches and also developed their own model.

According to the developments performed by Zhang [4], for a given penetration δ, the resistance of superelement number k is to be taken as

$$P_t^{(k)} = \frac{\sigma_0 t_w^{(k)}}{\sqrt{3}} \left(b_1^{(k)} + b_2^{(k)} \right) \cdot \left(\frac{t_w^{(k)}}{\sqrt{H\delta}} + \frac{4}{3} \frac{H\delta}{b_1^{(k)} b_2^{(k)}} \right), \qquad (4.3)$$

where $t_w^{(k)}$ is the web thickness of superelement k. In this formula, H is a parameter fixed by minimizing the mean crushing resistance over one fold. By so doing, Zhang [4] found that

$$H = \sqrt[3]{\frac{3\pi}{16} b_1^{(k)} b_2^{(k)} t_w^{(k)}}. \qquad (4.4)$$

4.3. Total Resistance in Local Deforming Mode

The total resistance of the gate in the local deforming mode is simply obtained by summing the individual contributions of the n superelements:

$$P_{\text{loc}} = \sum_{k=1}^{n} P_t^{(k)}. \qquad (4.5)$$

Of course, for a given value of δ, if a superelement has not been activated, it will not provide any resistance to the total resistance, and so we have

$$P_t^{(k)} = 0. \qquad (4.6)$$

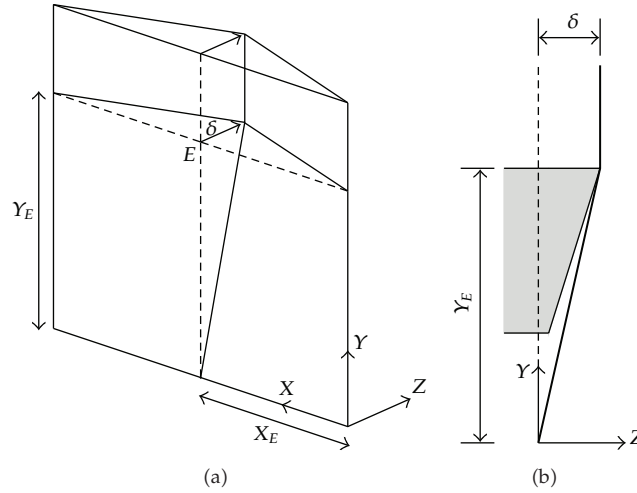(a)   (b)

Figure 17: (a) Assumed displacements field. (b) Displacement profile in the plan $X = X_E$.

5. Evaluation of the Resistance in the Global Deforming Mode

5.1. Displacements Fields

When the global mode is activated, the gate is assumed to undergo a global motion involving the entire structure. The displacements field obtained in this case is plotted in Figure 17(a). As mentioned earlier, the first contact between the bow and the plating is located in point E, with coordinates $(X_E, Y_E, 0)$. In the vertical plan passing through this point (i.e., the plan with equation $X = X_E$), we suppose that the displacements are distributed along the vertical Y axis as shown in Figure 17(b). The mathematical formulation of this profile is as follows:

$$W_E(Y, \delta) = \begin{cases} \delta \cdot \dfrac{Y}{Y_E} & \text{if } 0 \le Y < Y_E, \\ \delta & \text{if } Y_E \le Y \le H, \end{cases} \tag{5.1}$$

where W_E indicates that we consider the displacement in the plan $X = X_E$.

The two previous formulae are only valid as long as there is no other contact between the ship and the gate. However, as the vessel is moving forward, another contact will appear between the plating and the lowermost deck (see Figure 18). The particular value of δ for which this situation will occur is denoted by δ_c, and we have

$$\delta_c = Y_E \cdot \cot \phi, \tag{5.2}$$

where ϕ is the stem angle. When $\delta \ge \delta_c$, the contact between the bow and the plating is completely developed along the height h_b (see Figure 18). Consequently, it is required to
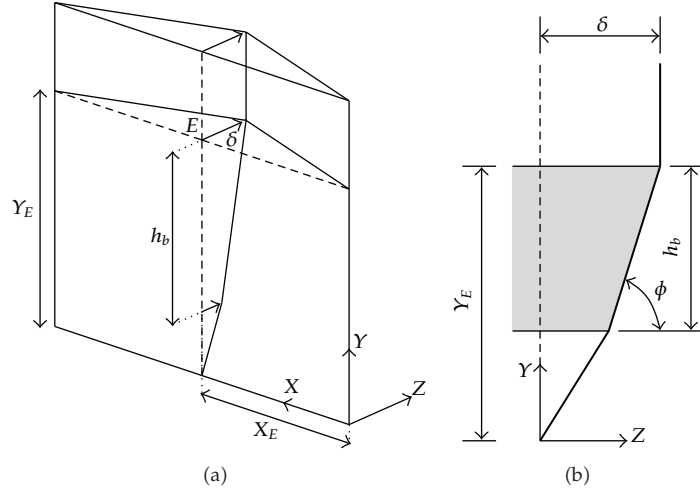
(a)   (b)

Figure 18: Assumed displacements field after second contact between the bow and the plating.

adapt the previous displacements fields in order to account for this phenomenon. Then, for $\delta \geq \delta_c$, we will use the following equations:

$$
W_E(Y, \delta) =
\begin{cases}
(\delta - h_b \cot \phi) \cdot \dfrac{Y}{Y_E - h_b} & \text{if } 0 \leq Y < Y_E - h_b, \\
\delta + (Y - Y_E)\cot \phi & \text{if } Y_E - h_b \leq Y < Y_E, \\
\delta & \text{if } Y_E \leq Y \leq H.
\end{cases}
\tag{5.3}
$$

5.2. Mechanical Model of the Gate

In the previous section, we have postulated a kinematically admissible displacements field. In accordance with the upper-bound method, it is now possible to use the principle of virtual velocities in order to estimate the resistance of the structure deformed in the global mode.

Unfortunately, it is rather difficult to derive analytically the resistance of a gate submitted to the displacements given by (5.1), (5.3). In order to simplify the problem, we make the assumption that *the main contribution to the resistance is coming from the bending of the gate between the two lock walls*. This hypothesis seems to be reasonable for a global mode, especially when the ratio H/L is wide, but we have to bear in mind that it may not remain valid in some special cases. As a consequence, the resistance in the global deforming mode is mostly provided by transversal frames, the stiffeners. Therefore, the gate may be seen as a set of independent beams subjected to a given displacements field. The contribution of the vertical frames is only to apply the expected displacements to these beams; we suppose that they do not take part mechanically in the resistance. According to these hypotheses, we obtain the equivalent model of the gate depicted in Figure 19.

The previously mentioned beams have a cross-section obtained by taking the gross cross-section of the transversal frames, to which the collaborating part of the plating is added (see the picture at the top of Figure 19). The values of h_f, t_f, h_w, t_w, and t_p are defined as
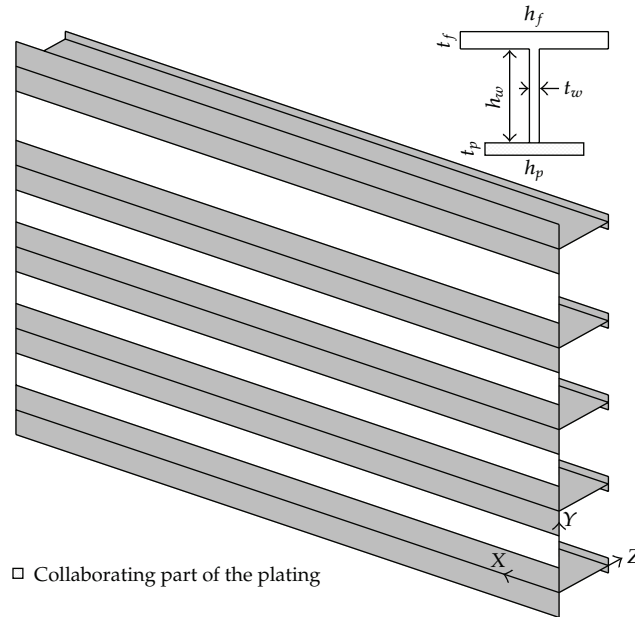
Figure 19: Mechanical model of the gate for assessing the resistance in the global deforming mode.

an input of the calculation process, but the collaborating length b_f has to be chosen in order to account for the following phenomena:

> (i) the shear lag effect occurring at the junction between the plating and webs of transversal frames;
>
> (ii) the overall buckling of the stiffened panel located between two transversal frames; this situation corresponds to the configuration (a) plotted in Figure 20.
>
> (iii) the local buckling of the plating located between two stiffeners; this is illustrated by the configuration (b) in Figure 20.

The calculation of the effective width b_{eff} (see Figure 20) on both sides of each transversal frame can be achieved by applying the rules provided by Eurocode 3 for longitudinally stiffened plates.

Finally, in order to achieve the mechanical modeling of the gate, we still have to give some details about the support conditions of the beams. As they are connected to the vertical frames, they will be mostly restrained at two levels:

> (i) a rotational restriction along the transversal X axis, which will hinder the torsional effects in the beams;
>
> (ii) a translational restriction along the longitudinal Z axis, which will hinder out-of-plane shearing and bending of the beams.

Of course, it is rather difficult to precisely account for these effects in an analytical procedure. As we are not trying to have an accurate resistance of the gate (but a good approximation), it is admissible to consider that each beam is simply supported at both ends. By so doing, we completely omit the additional restrains provided by the vertical frames, which is a conservative hypothesis for evaluating globally the impact resistance.
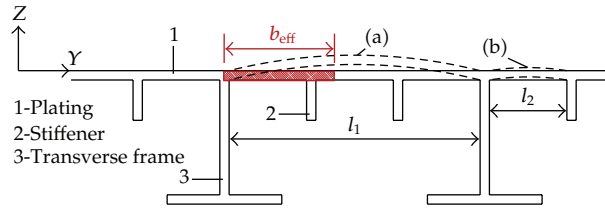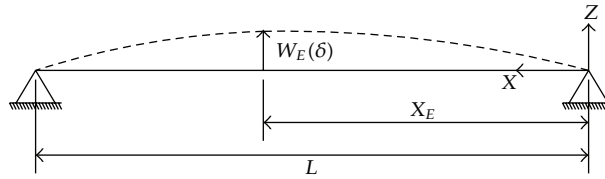
Figure 20: Calculation of the effective width.

Figure 21: Elastic deformation of a transversal frame.

5.3. Elastic Resistance

The mechanical model presented here is a set of n beams submitted to the displacements fields detailed in Section 5.1. In this section, we use the superscript (k) in order to refer to a particular beam, with $k \in \{1, 2 \dots, n\}$. At the beginning of the impact, a beam located at any given vertical position $Y^{(k)}$ is deformed according to the classical bending theory (see Figure 21). The deflected shape is then given by a parabola:

$$
W^{(k)}(X, \delta) = \begin{cases} \dfrac{X}{X_E} \dfrac{X^2 + X_E^2 - 2LX_E}{2X_E(X_E - L)} \cdot W_E^{(k)}(\delta) = f_1(X) \cdot W_E^{(k)}(\delta) & \text{if } 0 \leq X < X_E, \\[3mm] \dfrac{X - L}{X_E - L} \dfrac{X^2 + X_E^2 - 2LX_E}{2X_E(X_E - L)} \cdot W_E^{(k)}(\delta) = f_2(X) \cdot W_E^{(k)}(\delta) & \text{if } X_E \leq X < L, \end{cases}
\tag{5.4}
$$

where $W_E^{(k)}(\delta) = W_E(Y^{(k)}, \delta)$ and has been defined in Section 5.1. The curvature $\chi^{(k)}$ and the bending moments $M^{(k)}$ are obtained using the two following well-known relations:

$$
\chi^{(k)} = \frac{\partial^2 W}{\partial X^2}, \qquad M^{(k)} = EI^{(k)} \frac{\partial^2 W}{\partial X^2},
\tag{5.5}
$$

where E is the elastic modulus and $I^{(k)}$ is the bending inertia of beam k.

If we only consider the deformation energy arising from the bending of beam k, the internal power defined by (3.4) can be calculated by

$$
\dot{E}_{\text{int}}^{(k)} = \int_0^L M^{(k)} \dot{\chi}^{(k)} dX = EI\dot{\delta}W_E^{(k)}(\delta) \frac{\partial W_E^{(k)}}{\partial \delta} \left(\int_0^{X_E} \left(\frac{\partial^2 f_1}{\partial X^2} \right)^2 dX + \int_{X_E}^{L-X_E} \left(\frac{\partial^2 f_2}{\partial X^2} \right)^2 dX \right).
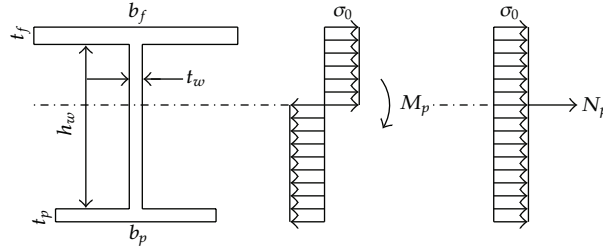\tag{5.6}
$$

Figure 22: Plastic properties of the cross-section.

By introducing (5.4) into (5.6), the individual contribution of beam k to the elastic resistance of the gate in the global deforming mode is defined by

$$P_t^{(k)} = EI^{(k)}W_E^{(k)}(\delta)\frac{\partial W_E^{(k)}}{\partial \delta} \cdot \frac{3L}{X_E^2(X_E - L)^2}. \tag{5.7}$$

5.4. Plastic Resistance

Of course, (5.7) remains valid as long as there is no plastic effect in beam k. However, when it is bent beyond its elastic limit, the transversal frame exhibits another kind of behavior, which may be described by using the two following properties:

(i) $M_p^{(k)}$: the plastic bending moment of beam k, corresponding to a complete plastic cross- section in bending (see Figure 22(a));

(ii) $N_p^{(k)}$: the normal plastic force of beam k, corresponding to a complete plastic cross-section in traction or compression (see Figure 22(b)).

With these properties, a classical plastic analysis may be performed. As soon as $M_p^{(k)}$ is reached, the section located in $X = X_E$ behaves like a plastic hinge and the structure becomes a mechanism. At this moment, the yield locus characterizing the cross-section is reached. However, it does not mean that the resistance is not increasing anymore. As the deformations are increasing, tensile stresses appear inside the beam k, and the cross-section is submitted to both a normal force $N^{(k)}$ and a bending moment $M^{(k)}$. As they are linked by the equation of the yield locus, these two actions are not independent.

In order to evaluate $M^{(k)}$ and $N^{(k)}$ for each of the n beams representing the gate, we need more information about plastic interaction. Yukio and Rashed [15] have elaborated a very refined description of the yield locus for the cross-section depicted in Figure 22. However, as suggested by Paik [11], it is easier to adopt a parabolic interaction criterion for beam number k (see Figure 23),

$$\frac{M^{(k)}}{M_p^{(k)}} + \left[\frac{N^{(k)}}{N_p^{(k)}}\right]^2 = 1 \Longleftrightarrow M^{(k)} = M_p^{(k)} - M_p^{(k)}\left[\frac{N^{(k)}}{N_p^{(k)}}\right]^2. \tag{5.8}$$
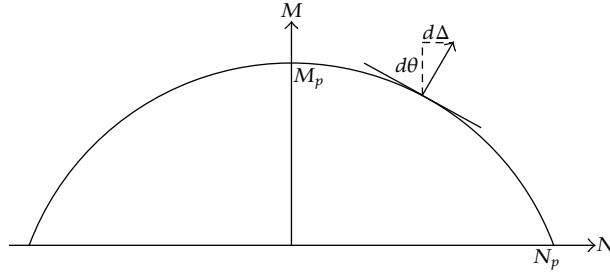
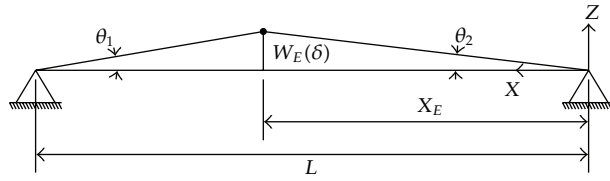**Figure 23:** Parabolic interaction criterion.

Figure 24: Plastic deformation of a transversal frame.

If we note $\Delta^{(k)}$ and $\theta^{(k)}$, the axial extension and the rotation in beam k, the required condition of normality is verified for the present yield locus if we have (see Figure 23)

$$\frac{dM^{(k)}}{dN^{(k)}} = -\frac{d\Delta^{(k)}}{d\theta^{(k)}} = -\frac{\dot{\Delta}^{(k)}}{\dot{\theta}^{(k)}} \Longleftrightarrow -\frac{2M_p^{(k)}N^{(k)}}{\left(N_p^{(k)}\right)^2} = -\frac{\dot{\Delta}^{(k)}}{\dot{\theta}^{(k)}}. \tag{5.9}$$

The extensional rate and rotational rates $\dot{\Delta}^{(k)}$ and $\dot{\theta}^{(k)}$ in beam k may be easily calculated by geometrical considerations based on Figure 24:

$$\dot{\theta}^{(k)} = \left(\frac{1}{X_E} + \frac{1}{L - X_E}\right)\frac{\partial W_E^{(k)}}{\partial \delta}\dot{\delta}, \qquad \dot{\Delta}^{(k)} = W_E(\delta)\frac{\partial W_E^{(k)}}{\partial \delta}\left(\frac{1}{X_E} + \frac{1}{L - X_E}\right)\dot{\delta}. \tag{5.10}$$

By introducing (5.10) into (5.9), we finally get a second relation between $M^{(k)}$ and $N^{(k)}$. We then obtain the classical formula giving the membrane force in an axially restrained beam:

$$N^{(k)} = \frac{\left(N_p^{(k)}\right)^2 W_E^{(k)}}{2M_p^{(k)}}. \tag{5.11}$$

At this stage, it is important to note that this result implies that the beam is perfectly restrained in the axial direction. This hypothesis implies that no transversal motions (along direction X) occur at the supports where $X = 0$ and $X = L$. This seems quite reasonable for the gate under consideration because of the action of vertical frames. However, it is important to keep in mind that we have formulated such an assumption because even small displacements may reduce considerably the present foreseen resistance.

The previous relation (5.11) is useful for isolating the associated bending moment $M^{(k)}$ in (5.8). By so doing, we get:

$$M^{(k)} = M_p^{(k)} - M_p^{(k)} \left(\frac{N_p^{(k)} W_E^{(k)}}{2 M_p^{(k)}} \right)^2. \tag{5.12}$$

The two previous equations are only valid if $N^{(k)} \leq N_p^{(k)}$ because it is impossible to exceed the total plastic capacity of the cross-section. Consequently, according to (5.11), the two mentioned equations may still be used as long as:

$$W_E^{(k)} \leq \frac{2 M_p^{(k)}}{N_p^{(k)}}. \tag{5.13}$$

If this limit displacement is exceeded in beam k, we simply have $N^{(k)} = N_p^{(k)}$ and $M^{(k)} = 0$. Once all internal forces and displacements field are completely defined, the upper-bound theorem is applied for getting the plastic collision resistance of beam k. According to Jones [16], the internal power of a transversal frame may be written as

$$\dot{E}_{\text{int}}^{(k)} = \int_0^L \left(M^{(k)} \dot{\theta}^{(k)} + N^{(k)} \dot{\Delta}^{(k)} \right) \cdot dX. \tag{5.14}$$

By introducing (5.10), (5.11), and (5.12) in (5.14), we finally get the individual contribution of beam k to the plastic resistance of the gate in the global deforming mode:

$$P_t^{(k)} = \begin{cases} \dfrac{L}{X_E (L - X_E)} M_p^{(k)} \dfrac{\partial W_E^{(k)}}{\partial \delta} \cdot \left[1 + \left(\dfrac{N_p^{(k)} W_E^{(k)}}{4 M_p^{(k)}} \right)^2 \right] & \text{if } W_E^{(k)} \leq \dfrac{2 M_p^{(k)}}{N_p^{(k)}}, \\[4mm] N_p^{(k)} \dfrac{L}{X_E (L - X_E)} W_E^{(k)} \dfrac{\partial W_E^{(k)}}{\partial \delta} & \text{if } W_E^{(k)} > \dfrac{2 M_p^{(k)}}{N_p^{(k)}}. \end{cases} \tag{5.15}$$

5.5. Total Resistance in Global Deforming Mode

In Sections 5.3 and 5.4, we have established the individual contribution of each transversal frame to the total resistance of the gate. In accordance with (3.12), the total collision force is simply obtained by summation:

$$P_{\text{glob}} = \sum_{k=1}^n P_t^{(k)}, \tag{5.16}$$

where $P_t^{(k)}$ is given by (5.7) if beam k is still in the elastic regime or by (5.16) if plasticity has already occurred. To simplify, the transition between the elastic and the plastic resistance is
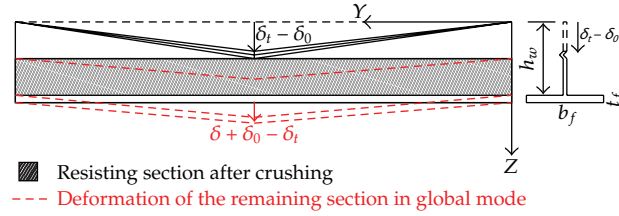
Figure 25: Resistance in the global mode of a transversal frame already crushed during the local mode.

supposed to happen when the elastic bending moment in section $X = X_E$ reaches its maximal value $M_p^{(k)}$.

6. Combination of Local and Global Deforming Modes

6.1. Resistance of the Beams Already Impacted during the Local Phase

The transition between local and global deforming mode has already been discussed in Section 3.4, where a sudden switch is assumed to occur when $\delta = \delta_t$ (the so-called transition value). In the present section, we give more precision on the way to combine two different modes. For a given value of δ, P_{loc} is evaluated by (4.5) and P_{glob} by (5.16). Two cases are then possible.

- (i) If $P_{\text{loc}} > P_{\text{glob}}$, then the force applied by the ship on the gate is not sufficient for activating the global deforming mode. Consequently, we have $\delta < \delta_t$ and $P_t = P_{\text{loc}}$, with P_{loc} given by (4.5).

- (ii) If $P_{\text{glob}} = P_{\text{loc}}$, then the global bending mode is activated and the gate starts to resist by an overall movement. So we have $\delta = \delta_t$; the transition value is reached.

For $\delta \geq \delta_t$, we know that the global mode is valid, but the resistance P_t may no longer be evaluated by relation (5.16). If we examine Figure 26, for example, we see that when the transition occurs at δ_t, the third transversal frame has already been crushed over a certain length $\delta_t - \delta_0$, where δ_0 is the initial distance between the bow and the frame. As a consequence, for beam 3, we may not assume that (5.7) and (5.15) are still valid.

It is too conservative to suppose that a beam that has already been crushed during the local phase does not provide any resistance during the global one. On the contrary, the uncrushed part of the cross-section is still able to develop a certain resistance by acting like a membrane. This is illustrated in Figure 25, where, for beam k, we see that the total area of the uncrushed section is

$$A_r^{(k)} = \left(h_w^{(k)} + \delta_0^{(k)} - \delta_t \right) t_w^{(k)} + b_f^{(k)} t_f^{(k)}, \tag{6.1}$$

where $h_w^{(k)}$, $t_w^{(k)}$, $b_f^{(k)}$, and $t_f^{(k)}$ are the cross-sectional dimensions for beam k, $\delta_0^{(k)}$ is the initial distance between the bow and beam k.
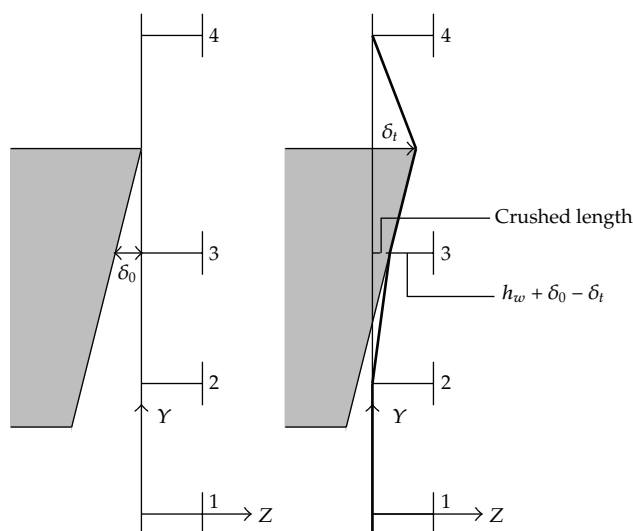
Figure 26: Combination of local and global deforming modes.

When $\delta > \delta_t - \delta_0$, the internal power developed while producing an additional displacement $\delta + \delta_0 - \delta_t$ of beam k is

$$\dot{E}_{\text{int}} = \sigma_0 A_r^{(k)} \dot{\Delta}^{(k)}, \tag{6.2}$$

where $\Delta^{(k)}$ is the axial extension of the transversal frame caused by the displacement $\delta + \delta_0 - \delta_t$:

$$\Delta^{(k)} = \frac{L}{2} \cdot \frac{\left(\delta + \delta_0^{(k)} - \delta_t\right)^2}{X_E(L - X_E)} \iff \dot{\Delta}^{(k)} = L \cdot \frac{\delta + \delta_0^{(k)} - \delta_t}{X_E(L - X_E)} \dot{\delta}. \tag{6.3}$$

Finally, by introducing (6.3) into (6.2), we obtain the resistance of a transversal frame already crushed during the local phase:

$$P_t^{(k)} = \sigma_0 A_r^{(k)} L \cdot \frac{\delta + \delta_0^{(k)} - \delta_t}{X_E(L - X_E)}. \tag{6.4}$$

Of course, this formula has only to be applied if $\delta_t \geq \delta_0^{(k)}$, otherwise beam k is not impacted during the local mode and the classic formulae of Section 5 remains valid. However, a correction is still needed to take into account the beginning of a new phase of motion. In fact, in (5.7) and (5.15), we have to evaluate $W_E^{(k)}$ and $\partial W_E^{(k)}/\partial \delta$ for the actual *global* displacement, that is, $\delta - \delta_t$ and not for the *total* displacement δ, which also includes the displacements during the local phase. This concept is illustrated in Figure 27.
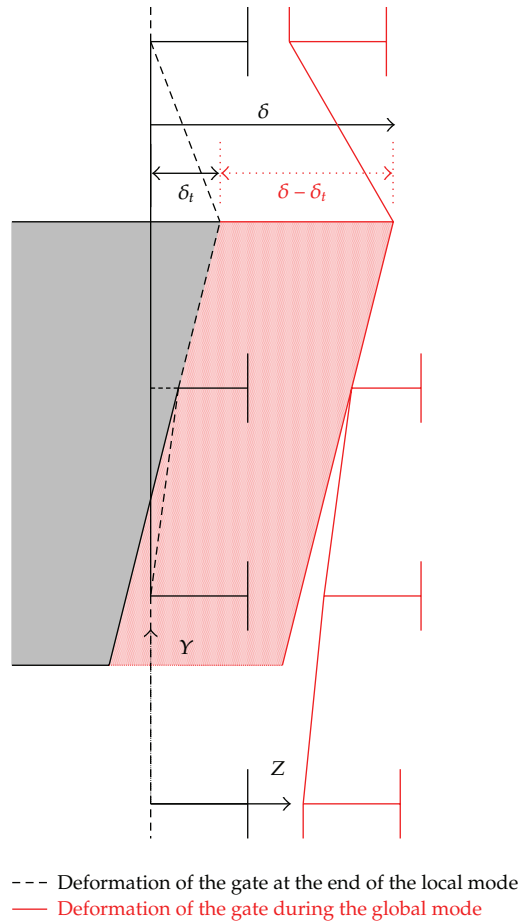
--- Deformation of the gate at the end of the local mode
—— Deformation of the gate during the global mode

Figure 27: Total displacement δ and global displacement $\delta - \delta_t$.

6.2. Total Resistance

In the previous sections, we have established all the required formulas for assessing the resistance in the local and global deforming modes. For clarity, we will now make a short summary of the results.

(1) At the beginning, the progression of the striking vessel into the gate is allowed by local deformations of the structure. During this local phase, two different forces are evaluated:

$P_{\text{loc}}(\delta) \rightarrow$ see formula (4.5) where $P_t^{(k)}$ is given by

(i) formula (4.2) if superelement k is of type 1,
(ii) formula (4.3) if superelement k is of type 2,

$P_{\text{glob}}(\delta) \rightarrow$ see formula (5.16), where $P_t^{(k)}$ is given by

(i) formula (5.7) if beam k is still in the elastic regime,
(ii) formula (5.15) if beam k is in the plastic regime.

During the local phase, the total resistance of the gate P_t is equal to the local one, which means that $P_t(\delta) = P(\delta)$.

We assume that deformations remain local as long as $P_{\text{glob}}(\delta) > P_{\text{loc}}(\delta)$. The transition between the local and the global mode occurs at the particular value δ_t, for which we have $P_{\text{glob}}(\delta_t) = P_{\text{loc}}(\delta_t)$.

(2) For the values of δ greater than δ_t, the global mode is activated. The total resistance of the gate is still given by

$$P_t(\delta) = P_{\text{loc}}(\delta_t) + \sum_{k=1}^{n} P_t^{(k)}, \tag{6.5}$$

where

  (i) P_t^k is obtained by formula (5.7) or formula (5.15) if beam k has not been impacted during the local phase; it should be noted that these equations are evaluated in $\delta - \delta_t$ and not in δ (see Figure 27),
  (ii) P_t^k is obtained by formula (6.4) if beam k has been impacted during the local deforming mode,
  (iii) $P_{\text{loc}}(\delta_t)$ is the total resistance of the gate at the end of the local phase.

7. Numerical Validation

In order to validate all the developments described in the previous sections, we compare them to the results obtained by numerical simulations on two different gates. For each studied lock gate, two situations of collision have been considered: in the first case, the impact point E is located in the upper part of the gate; in the second case, it is positioned in the lower part.
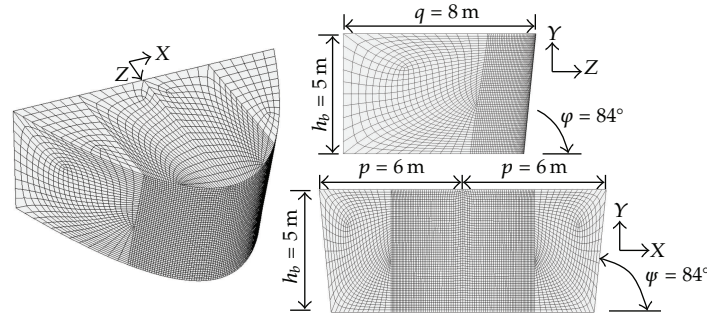
7.1. Numerical Model of the Striking Vessel

As mentioned above, we are only interested by the worst damages that may be caused to the gate during the collision. So far, we are not concerned by the destruction of the striking vessel. Therefore, we conservatively assume that the ship is perfectly rigid and will not deform over the total impact duration.

For the numerical simulations, it is useless to deal with the entire ship. We only need to have a quite refined model of the bow. As explained in Section 2, the geometry of the ship is fixed with help of the five parameters p, q, φ, ψ, and h_b (see Figure 28). Its mass M_0 is noted and its initial velocity V_0. For the present example, we have chosen the numerical values listed in Table 1. These parameters have been chosen in order to represent a classical ship for the inland waterways.

The numerical model of the vessel is shown in Figure 28. It is composed of 6955 Belytschko-Tsai shell elements, which are described in the LS-DYNA theoretical manual by Hallquist [17]. As it can be seen in Figure 28, the mesh is more refined in the central zone of the ship, where the contact with the gate is likely to occur. In this region, the mesh size is about 1 cm × 1 cm. In the remaining parts of the model, as they are not supposed to develop any contact with the impacted structure, the mesh is coarser.

Table 1: Numerical data describing the striking vessel.

p	q	φ	ψ	h_b	M_0	V_0
6 m	8 m	84°	84°	5 m	4000 t	2 m/s

Figure 28: Numerical model of the striking vessel.

Table 2: Useful properties for defining a rigid material law (only required for contact simulation).

Property	Notation	Value
Density	ρ	7850 kg/m³
Young's modulus	E_Y	210 000 MPa
Poisson's ratio	ν	0.33

The material used for modeling the bow is assumed to be rigid. It is defined with help of the classical properties of steel recalled in Table 2. These parameters are only required for defining the contact conditions between the ship and the gate. They are not used for calculating any deformation in the vessel, as the material is infinitely rigid.

7.2. Numerical Model of Gate 1

The main dimensions of the structure are plotted in Figure 29. The total height and length of the gate are $H = 13.1$ m and $L = 13.1$ m. The stiffening system of the structure is made of

  (i) five transversal frames, which are irregularly distributed over the height H of the gate; their vertical positions along the vertical Y axis are shown in Figure 29(b);

  (ii) six vertical frames, which are regularly placed over the length L of the gate; their locations along the transversal X axis are plotted in Figure 29(c);

  (iii) twenty stiffeners distributed over the height H of the gate with an average space of 66 cm.

Other geometrical data are listed in Table 3. The corresponding notations are defined in accordance with the symbols introduced in Figure 3. Note that the transversal and vertical frames have a T-shaped cross-section, while the stiffeners simply have a rectangular one. The gate is modeled with help of 204226 Belytschko-Tsai shell elements. The mesh is quite refined, with a mesh size of 5 cm × 5 cm. Of course, it may appear excessive to use such a regular mesh over the entire structure, but it was required because we did not know in advance which part
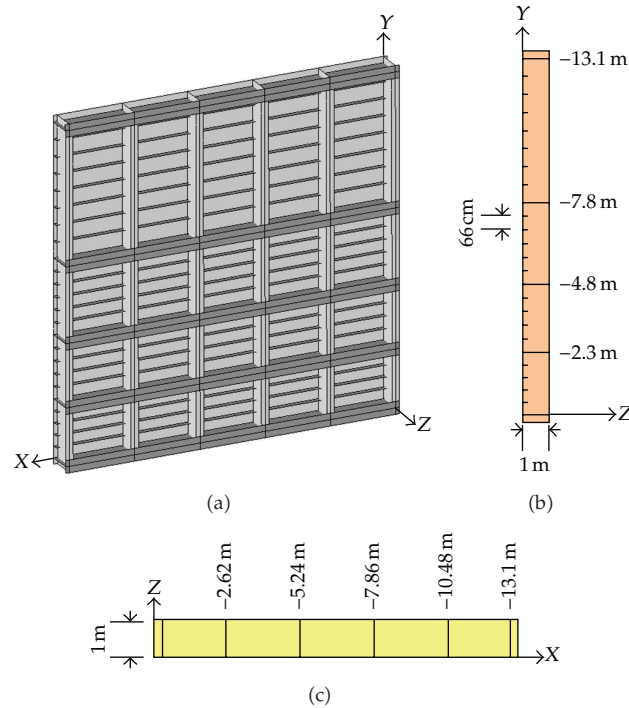
(a)

(b)

(c)

Figure 29: Numerical model of gate 1.

Table 3: Geometrical data defining gate 1.

Element	Property	Notation	Value (mm)
Plating	Thickness	t_p	10
Transversal frames	Web thickness	t_w	22
	Web height	h_w	1000
	Flange thickness	t_f	22
	Flange width	b_f	300
Vertical frames	Web thickness	t_w	22
	Web height	h_w	1000
	Flange thickness	t_f	22
	Flange width	b_f	500
Stiffeners	Web thickness	t_w	10
	Web height	h_w	200
	Flange thickness	t_f	0
	Flange width	b_f	0

of the gate would be impacted by the ship. In order to avoid contact problems, this solution has been chosen.

The material used for gate 1 is defined to represent more or less the behaviour of steel. The elastic-plastic stress-strain curve may be divided in two distinct portions (see Figure 30). The first part of the curve corresponds to the elastic phase. The stress-strain curve is linear, with an inclination corresponding to Young's Modulus E_Y. When the yield stress
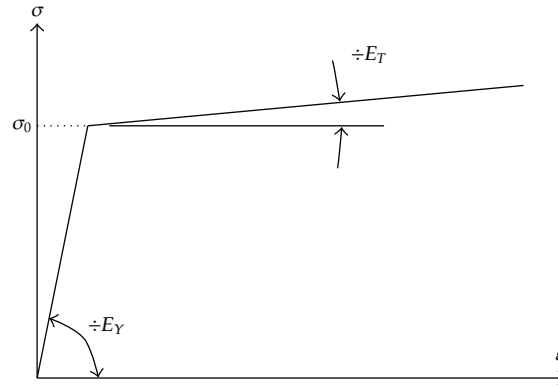
Figure 30: Stress-strain relation of steel.

Table 4: Useful properties for defining the material law of steel.

Property	Notation	Value
Density	ρ	$7850 \, \text{kg/m}^3$
Poisson's ratio	ν	0.33
Yield stress	σ_0	240 MPa
Young's modulus	E_Y	210 000 MPa
Tangent modulus	E_T	1018 MPa

σ_0 is reached, the plastic phase begins. The stress-strain curve is still linear, but the slope has changed and is given by the tangent modulus E_T. In the present low velocity impact model, the strain-rate effect is not taken into account. The values of the different parameters are listed in Table 4.

The support conditions are the ones described in Section 2, that is, displacements in direction Z are blocked in $X = 0$, $X = L$, and $Y = 0$.

7.3. Numerical Model of Gate 2

The second gate is wider than the first one. Its total height and length are $H = 15$ m and $L = 17.1$ m. The main dimensions are plotted in Figure 31. (Please note that the origin of the axes (X, Y, Z) is correctly positioned, regarding all the previous figures.) This time, the stiffening system is more compact and made of

(i) five transversal frames, whose vertical positions along the Y axis are shown on Figure 31;

(ii) six vertical frames, regularly separated by a distance of 1.9 m;

(iii) twenty-six stiffeners, regularly separated by a distance of 50 cm.

Other geometrical data are listed in Table 6. The gate is modeled by 92671 Belytschko-Tsai shell elements. The regular mesh size is 10 cm × 10 cm. The material model and the support conditions are the same as for gate 1.
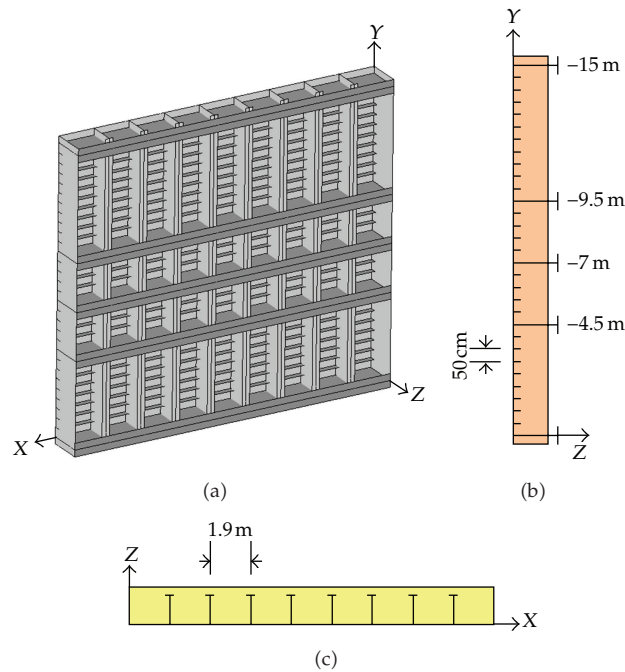
(a) (b)

(c)

Figure 31: Numerical model of gate 2.

Table 5: Impact location for the simulations.

	Simulation 1	Simulation 2
Gate 1	$X_E = 6.55$ m	$X_E = 6.55$ m
	$Y_E = 8$ m	$Y_E = 13.1$ m
Gate 2	$X_E = 8.55$ m	$X_E = 8.55$ m
	$Y_E = 7.5$ m	$Y_E = 13.25$ m

7.4. Numerical Simulations

Four numerical simulations have been performed by using the finite-elements software LS-DYNA. Two simulations are required for each gate, according to the position of the impact point E. The transversal and vertical positions X_E and Y_E of point E are listed in Table 5 for the different collision cases considered here.

Concerning the resulting crushing force curves compared in Figures 32 and 33, simulation 1 corresponds to a ship impact happening in the lower part of the structure and simulation 2 to an impact in the upper one.

7.5. Comparison of Numerical and Analytical Results

In order to validate the analytical developments established in the previous section, we will make a comparison between the results provided by LS-DYNA and the ones predicted by our simplified method. The curves of interest are those showing the evolution of the crushing force P_t with the total penetration δ. The comparisons are plotted in Figures 32 and 33.
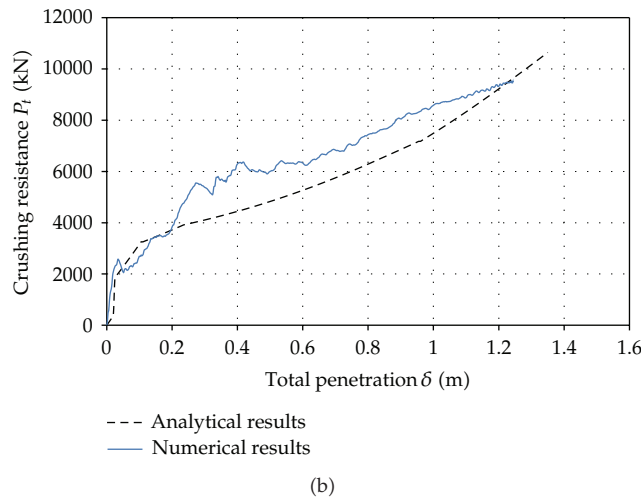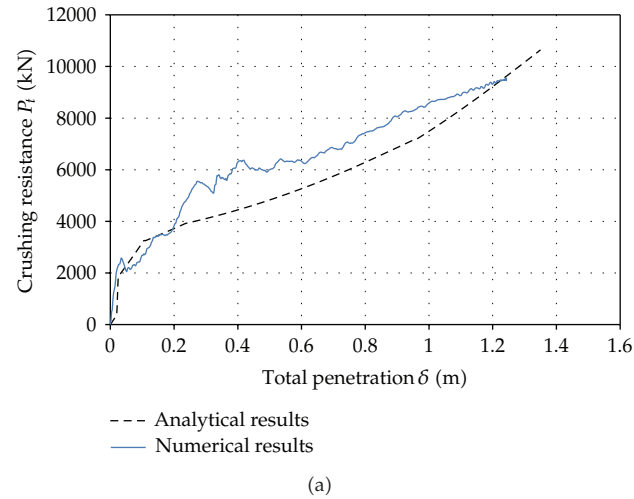
(a)

(b)

Figure 32: Comparison of the analytical and numerical crushing forces for gate 1.

The curves referenced as "numerical results" are those obtained by LS-DYNA, while the "analytical results" are derived by the present simplified approach.

As it can be seen, the agreement between the curves is quite good. In most cases, the analytical curves provide slightly conservative results. However, for gate 2, the first simulation (see Figure 33(a)) exhibits a more important divergence: our simplified method tends to underestimate the crushing resistance, especially for the great values of δ. This observation is due to a quite conservative approach in the global mode. This may be explained by the two following reasons.

(i) The resisting cross-sections are determined according to the recommendations of Eurocode 3. It seems that these rules are quite severe in the present case as the numerical simulations show that a greater part of the plating is actually collaborating to the resistance of the transversal frames.

Table 6: Geometrical date defining gate 2.

Element	Property	Notation	Value (mm)
Plating	Thickness	t_p	12
Transversal frames	Web thickness	t_w	12
	Web height	h_w	1800
	Flange thickness	t_f	12
	Flange width	b_f	400
Vertical frames	Web thickness	t_w	12
	Web height	h_w	1400
	Flange thickness	t_f	12
	Flange width	b_f	300
Stiffeners	Web thickness	t_w	12
	Web height	h_w	300
	Flange thickness	t_f	0
	Flange width	b_f	0

(ii) We do not capture properly the deformation pattern of the vertical frames: we suppose that their role is limited to the application of the global displacements field, but we neglect the energy also dissipated through their own global deflection.

This last point is confirmed by the curves plotted on Figure 34, where we compare the energy dissipated by the different structural components of the gate. The numerical results are those given by LS-DYNA, while the analytical results are those predicted by the theoretical model of this paper. As it can be seen on this picture, the discrepancy is satisfactory for the plating, the stiffeners, and the transverse frames, but it is not really the case for the vertical frames. Our method underestimates the energy that these elements really dissipate, but this approximation remains conservative.

8. Conclusion

In this paper, we exposed a simplified procedure for assessing the resistance of a gate submitted to a ship impact.

It is important to bear in mind the hypotheses that we have formulated for modeling the struck gate and the striking vessel. Concerning the struck gate, our approach is devoted to

(i) gates with single plating; structures with double plating or caissons are not covered by the present developments;

(ii) gates with a classical orthogonal stiffening system, that is, stiffeners and frames in the transversal direction and frames in the vertical direction;

(iii) gates supported on both sides by the lock walls and by a sill at the bottom of the lock.

The three former conditions have to be fulfilled for applying the methodology exposed previously. Concerning the striking vessel, it is modeled by using a certain number of parameters. The global bow shape is assumed to be a parabola, with given radii p and q, decreasing according to given stem and side angles φ and ψ.

The impacted structure is assumed to behave in two phases. At the beginning, when the indentation δ of the ship is not too wide, we suppose a localized crushing of some impacted structural elements. The plating and the stiffening system surrounding the initial
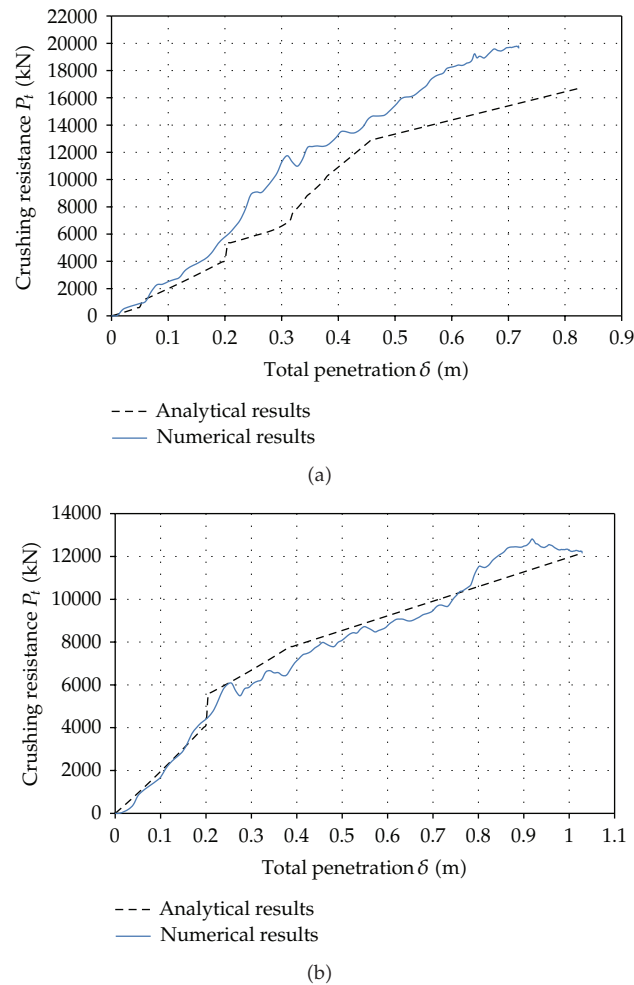
(a)

(b)

Figure 33: Comparison of the analytical and numerical crushing forces for gate 2.

contact zone are submitted to heavy deformations, but the remaining of the gate is still unaffected. In this case, we say that the structure withstands through a local deforming mode. For such a situation, the resistance is calculated by summing all the contributions of the activated superelements. As some references are already available in the literature, we have not reproduced all the developments concerning these superelements.

When the penetration δ becomes wider, the gate withstands through an overall movement implying the entire structure. In this case, we say that the resistance is provided through a global deforming mode. For the support conditions assumed presently, the required theoretical displacements fields have been exposed in detail. We also derived an equivalent mechanical model for evaluating the resistance in such a situation.

The transition between the local and the global deforming modes is assumed to occur at a given penetration δ_t, for which the collision force exerted by the ship during the local phase is sufficient to produce an overall displacement of the gate.

Finally, our presentation ends with a comparison between some finite elements numerical results and those obtained by the present simplified approach. In most cases, the
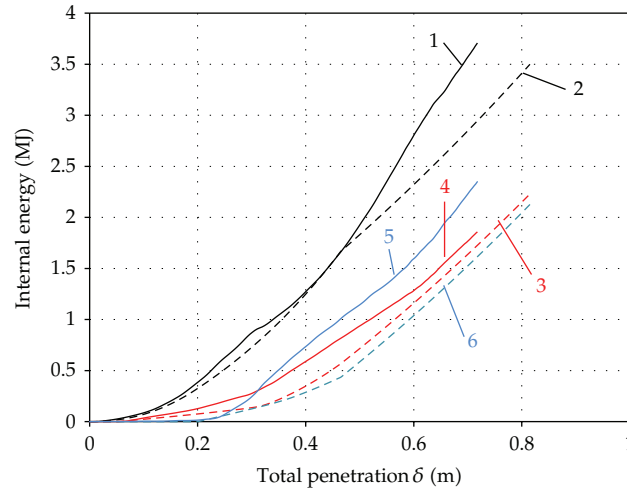
(1) Energy dissipated by the plating and the stiffeners (numerical results)
(2) Energy dissipated by the plating and the stiffeners (analytical results)
(3) Energy dissipated by the transverse frames (numerical results)
(4) Energy dissipated by the transverse frames (analytical results)
(5) Energy dissipated by the vertical frames (numerical results)
(6) Energy dissipated by the vertical frames (analytical results)

Figure 34: Comparison of the analytical and numerical internal energy of the various components of the gate.

procedure exposed here leads to a quite satisfactory estimation of the collision resistance. The predicted results are conservative, without underestimating too much the numerical values.

The main advantage of the methodology exposed here is to provide rapidly an evaluation of the collision resistance. The analytical curves plotted in Figures 32 and 33 are useful for knowing if a lock gate is able to behave satisfactorily to an impact of a ship with given initial velocity V_0 and mass M_0. With these curves, it is in fact possible to know the total needed indentation $\delta_{\max}$ required for dissipating the initial kinetic energy $M_0 V_0^2 / 2$. If this value of $\delta_{\max}$ exceeds a given criterion, then we may suppose that the structure will not be able to withstand satisfactorily a collision with a vessel of mass M_0 and velocity V_0.

Of course, we have to be conscious that our simplified analytical method is only applicable at the predesign stage of a lock. For more advanced stages of a project, it is still necessary to resort to more advanced tools, like finite elements software.

List of Notations

Lower-Case Latin Notations

a_1: Horizontal or vertical dimension of a superelement defined by the impact
point location and the supports of the struck structure
a_2: Horizontal or vertical dimension of a superelement defined by the impact
point location and the supports of the struck structure (complementary to a_1)
b_1: Vertical dimension of a superelement defined by the impact point location and
the supports of the struck structure

b_2:   Vertical dimension of a superelement defined by the impact point location and the supports of the struck structure (complementary to a_2)

b_{eff}:   Effective width for calculating the section properties of a transversal beam

b_f: Flange width of a stiffener or a transversal frame

h_b: Vertical distance between the lowermost and uppermost decks of the striking ship

h_p: Collaborating width of the plating in the global deforming mode

h_w: Web height of a stiffener or a transversal frame

k: Superscript used for referencing a particular property of superelement $n°k$

n: Total number of superelements used for modeling the entire gate

(p, q):   Parameters defining the parabolic dimensions of the striking ship uppermost deck

t_f: Flange thickness of a stiffener or a transversal beam

t_p: Thickness of the plating

t_w: Web thickness of stiffener or a transversal frame

t_X: Equivalent plating thickness after smearing all the transversal stiffeners

t_Y: Equivalent plating thickness after smearing all the vertical stiffeners.

Upper-Case Latin Notations

E: Young's modulus of the steel material constituting the gate

E_{ext}:   External energy

E_{int} Internal energy

E_T: Tangent modulus of steel

E_Y: Young's modulus of steel

H: Total vertical height of the gate

I: Bending inertia of a transversal beam

L: Total transversal length of the gate

M: Bending moment

M_p: Plastic bending resistance of a transversal beam

M_0:   Mass of the striking ship

N: Axial force

N_p: Plastic axial resistance of a transversal beam

P_{glob}:   Total resistance of the gate in the global deforming mode

P_{loc}:   Total resistance of the gate in the local deforming mode

P_t: Total collision resistance of the impacted gate

$W(X, \delta)$: Transversal evolution of the displacement field in the global deforming mode

$W_E(Y, \delta)$: Vertical evolution of the displacement field in the global deforming mode

(X_E, Y_E): Impact point location on the gate

(X, Y, Z): General coordinate system.

Lower-Case Greek Notations

δ: Penetration of the striking ship

δ_c: Penetration of the striking ship for which a second contact between the gate and the bow is established

δ_t: Penetration of the striking ship at the transition between the local and the global deforming modes

$\delta_{\max}$: Maximal penetration of the striking ship required for completely dissipating its initial kinetic energy

δ_0: Initial distance between the bow and a transversal beam

ϵ_u: Deformation for which the ultimate stress σ_u is reached

ϵ_0: Deformation for which the plastic limit σ_0 is reached

ϵ_{ij}: Strain tensor

θ: Cross-section rotation

ν: Poisson's ratio of steel

ρ: Mass density of steel

σ_u: Ultimate stress of steel

σ_0: Plastic limit of steel

σ_{ij}: Stress tensor

ϕ: Stem angle

χ: Curvature of a transversal beam

ψ: Side angle.

Upper-Case Greek Notations

Γ: Designation of the parabola describing the striking ship uppermost deck

Δ: Total axial extension of transversal frame.

References

[1] T. Wierzbicki and J. Culbertson Driscoll, "Crushing damage of web girders under localized static loads," *Journal of Constructional Steel Research*, vol. 33, no. 3, pp. 199–235, 1995.

[2] G. Wang and H. Ohtsubo, "Deformation of ship plate subjected to very large load," *Journal of Offshore Mechanics and Arctic Engineering*, vol. 119, 1997.

[3] B. C. Simonsen, "Ship grounding on rock—I. Theory," *Marine Structures*, vol. 10, no. 7, pp. 519–562, 1997.

[4] S. M. Zhang, *The mechanics of ship collisions*, Ph.D. thesis, Department of Naval Architecture and Offshore Engineering, Technical University of Denmark, 1999.

[5] L. Hong and J. Amdahl, "Crushing resistance of web girders in ship collision and grounding," *Marine Structures*, vol. 21, no. 4, pp. 374–401, 2008.

[6] G. Wang, "Some recent studies on plastic behavior of plates subjected to large impact loads," *Journal of Offshore Mechanics and Arctic Engineering*, vol. 124, no. 3, pp. 125–131, 2002.

[7] G. Wang and H. Ohtsubo, "An upper-bound solution to the problem of plate tearing," *Journal of Marine Science and Technology*, vol. 1, no. 1, pp. 46–51, 1995.

[8] S. Zhang, "Plate tearing and bottom damage in ship grounding," *Marine Structures*, vol. 15, no. 2, pp. 101–117, 2002.

[9] T. Wierzbicki, "Concertina tearing of metal plates," *International Journal of Solids and Structures*, vol. 32, no. 19, pp. 2923–2943, 1995.

[10] P. E. Zheng, *Theorical analysis of wedge cutting through metal plates*, Ph.D. thesis, Massachusetts Institute of Technology, 1994.

[11] J. K. Paik, *Ultimate Limit State Design of Steel-Plated Structures*, John Wiley and Sons, Chichester, UK, 2002.

[12] S. R. Cho and H. S. Lee, "Experimental and analytical investigations on the response of stiffened plates subjected to lateral collisions," *Marine Structures*, vol. 22, no. 1, pp. 84–95, 2009.

[13] Y. Ueda, S. M. H. Rashed, and J. K. Paik, "Buckling and ultimate strength interaction in plates and stiffened panels under combined inplane biaxial and shearing forces," *Marine Structures*, vol. 8, no. 1, pp. 1–36, 1995.

[14] H. Le Sourne, J. C. Rodet, and C. Clanet, "Crashworthiness analysis of a lock gate impacted by two river ships," *International Journal of Crashworthiness*, vol. 7, no. 4, pp. 371–396, 2004.

[15] U. Yukio and S. M. H. Rashed, "The idealized structural unit method and its application to deep girder structures," *Computers and Structures*, vol. 18, no. 2, pp. 277–293, 1984.

[16] N. Jones, *Structural Impact*, Cambridge University Press, 1997.

[17] J. O. Hallquist, *LS-DYNA Theoretical Manual*, Livermore Software Technology Corporation, 2006.